HHS Public Access

Author manuscript

Angiogenesis. Author manuscript; available in PMC 2022 February 01.

Published in final edited form as:

Angiogenesis. 2021 February ; 24(1): 177–190. doi:10.1007/s10456-020-09756-4.

Talin-Dependent Integrin Activation is Required for Endothelial Proliferation and Postnatal Angiogenesis

Fadi E. Pulous[1], **Jamie C. Carnevale**[1], **Zaki Al-Yafeai**[2], **Brenna H. Pearson**[2], **Jamie A.G. Hamilton**[1], **Curtis J. Henry**[1], **A. Wayne Orr**[2,3,4], **Brian G. Petrich**[1,5]

[1]Department of Pediatrics, Aflac Cancer and Blood Disorders Center, Emory University, Atlanta, GA

[2]Department of Molecular and Cellular Physiology, LSU Health Sciences Center, Shreveport, LA

[3]Department of Cell Biology and Anatomy, LSU Health Sciences Center, Shreveport, LA

[4]Department of Pathology and Translational Pathobiology, LSU Health Sciences Center, Shreveport, LA

Abstract

Integrin activation contributes to key blood cell functions including adhesion, proliferation and migration. An essential step in the cell signaling pathway that activates integrin requires the binding of talin to the β-integrin cytoplasmic tail. Whereas this pathway is understood in platelets in detail, considerably less is known regarding how integrin-mediated adhesion in endothelium contributes to postnatal angiogenesis. We utilized an inducible EC-specific talin1 knock-out mouse (Tln1 EC-KO) and talin1 L325R knock-in mutant (Tln1 L325R) mouse, in which talin selectively lacks the capacity to activate integrins, to assess the role of integrin activation during angiogenesis. Deletion of talin1 during postnatal days 1-3 (P1-P3) caused lethality by P8 with extensive defects in retinal angiogenesis and widespread hemorrhaging. Tln1 EC-KO mice displayed reduced retinal vascular area, impaired EC sprouting and proliferation relative to Tln1 CTRLs. In contrast, induction of talin1 L325R in neonatal mice resulted in modest defects in retinal angiogenesis and mice survived to adulthood. Interestingly, deletion of talin1 or expression of talin1 L325R in ECs increased MAPK/ERK signaling. Strikingly, B16-F0 tumors grown in Tln1 L325R adult mice were 55% smaller and significantly less vascularized than tumors grown in littermate controls. EC talin1 is indispensable for postnatal development angiogenesis. The role of EC integrin activation appears context-dependent as its inhibition is compatible with postnatal development with mild defects in retinal angiogenesis but results in marked defects in tumor growth and angiogenesis.

[5]**Address correspondence to:** Brian Petrich, Ph.D., Assistant Professor of Pediatrics, Aflac Cancer and Blood Disorders Center, Emory University School of Medicine, 2015 Uppergate Drive, Room 422, Atlanta, GA, 30322, Tel:(404) 727-0946, brian.petrich@emory.edu.

Disclosures:
None.

Inhibiting EC pan-integrin activation may be an effective approach to selectively target tumor blood vessel growth

Keywords

Talin1; Angiogenesis; Proliferation; Integrin

Introduction

Endothelial cells (ECs) form a tight, continuous monolayer of cells to form the luminal surface of blood vessels. ECs form adhesive contacts with the basement membrane at cell-matrix adhesions and are connected to neighboring cells at cell-cell contacts. In physiological contexts such as retinal angiogenesis but also in pathological contexts like tumor angiogenesis, ECs in pre-existing vessels facilitate new blood vessel growth by sensing and migrating towards soluble pro-angiogenic growth factors in their local microenvironment in a process broadly termed sprouting angiogenesis[1]. An essential activity during the early stages of sprouting angiogenesis necessitates the tight regulation of EC adhesive interactions with the extracellular matrix (ECM) as sprouting tip ECs navigate through the matrix[2,3]. ECs engage ECM components such as fibronectin, collagen and laminin through the integrin family of cell-surface adhesion receptors [4,5].

Integrins are heterodimeric, transmembrane receptors comprised of one of 18 α- and one of 8 β-subunits which in-turn dictate specificity for ligand. ECs express a diverse repertoire of integrin receptors with the best-studied receptors binding directly to collagen (α1β1, α2β1), fibronectin (α5β1, α4β1, αvβ3), vitronectin (αvβ3, avβ5) and laminin (α3β1, α6β1) [6,7]. Integrin receptors operate as bi-directional signaling hubs which transmit signals in both directions across the plasma membrane. Ligation of integrins to ECM ligands initiate intracellular signaling through so-called outside-in signaling which includes integrin clustering, recruitment of adapter proteins, kinases, phosphatases and reinforcement of integrin linkage to the actin cytoskeleton[8,9]. On one hand the affinity of integrins for extracellular ligands can be dynamically regulated by so-called inside-out signaling, or integrin activation, when intracellular signals, often downstream of growth factor receptor activation, initiate a signaling pathway that ultimately results conformational changes in the integrin extracellular domain associated with high ligand affinity. Indeed, integrin signaling thus functions in close coordination with growth factors like vascular endothelial growth factor (VEGF) [10-12] and fibroblast growth factor (FGF)[13,14] to drive a host of critical cell processes including migration, proliferation and survival[4,5].

Activation of integrin receptors into a high ligand affinity confirmation requires the binding of the cytoskeletal adaptor protein, talin, to the cytoplasmic tail of β-integrin [15-17]. An example of this conserved regulatory mechanism is observed in platelet adhesion during clot formation wherein soluble cues such as thrombin or adenosine diphosphate induce downstream signaling events which recruit talin to the plasma membrane allowing talin to activate the platelet receptors αIIbβ3 and α2β1[18,19]. Following these studies, several reports determined that ablation of talin1 in platelets impairs platelet adhesion during

hemostatic and thrombotic contexts while expression of a talin1 mutant which abrogates the MP binding interaction required for inside-out activation phenocopied the loss of talin[20,21]. While these studies have greatly informed therapeutic interventions for patients with defective platelet integrin signaling, the role of integrin affinity modulation in ECs has been relatively understudied.

The roles of specific integrin subunits in ECs during developmental and postnatal angiogenesis have been investigated and are reviewed concisely in other literature [22]. Indeed, studies utilizing individual integrin subunit deletion *in vivo* have been informative yet given the complex subunit-specific contributions as well as the context-dependent nature of these contributions much remains to be understood; specifically, in regards to whether inside-out integrin activation is essential for EC function in postnatal life. Early work determined the essential requirement of EC talin1 during embryonic angiogenesis as its deletion results in embryonic lethality by E10.5 due to extensive vascular defects[23] while inducible deletion of talin1 in established embryonic vessels results in early lethality due to defects in vascular permeability[24,25]. However, whether talin-mediated integrin activation is required for either pathological or physiological angiogenesis remains largely unanswered.

Here, we provide evidence to support the notion that talin and its role in activating integrins are indispensable for postnatal angiogenesis. Specifically, inducible deletion of EC talin1 during early postnatal development results in extensive defects in retinal angiogenesis, EC proliferation relative to littermate controls and early lethality of Tln1 EC-KO pups by P8. Deletion studies were complemented by an inducible, EC-specific talin1 L325R knock-in model to discern between integrin activation-dependent and independent contribution of talin in angiogenesis. Interestingly, whereas Tln1 L325R mice exhibited defects in retinal and tumor angiogenesis relative to littermate controls, induced expression of the mutant allele during postnatal development was not lethal, as was observed with Tln1 EC-KO mice, but resulted in significantly smaller mice that survive into adulthood. We observed elevated mitogen-activated protein kinase (MAPK) signaling upon talin1-depletion or expression of the talin1 L325R mutant suggesting that the observed defects in angiogenesis are at least in part dependent on dysregulated MAPK signaling in ECs. Our data point to an essential role for talin1 in postnatal angiogenesis although the specific contributions of integrin activation-dependent functions of talin require further investigation.

Methods

Mice

We generated EC-specific talin1 knock-out mice using *Tln1* floxed mice[18,19] expressing a tamoxifen-inducible Cre-recombinase driven by the cadherin 5 (*Cdh5*) promoter[26]. Our breeding scheme generated $Tln1^{f/f}$;Cdh5-CreERT2$^{-/-}$ (referred to as Tln1 CTRL) and $Tln1^{f/f}$;Cdh5-CreERT2$^{+/-}$ (Tln1 EC-KO) mice. For postnatal angiogenesis and developmental studies, mice were intragastrically administered 50μg of tamoxifen (Cayman Chemicals) dissolved in corn oil (Sigma) daily on P1-P3. For tumor studies in adult Tln1 Het/L325R mice, 8-10 week old mice were administered 2.5 mg of tamoxifen once daily for 3 days to induce L325R expression. Tln1 Het ($Tln1^{f/wt}$; Cdh5-CreERT2$^{+/-}$) and Tln1 L325R

(*Tln1*$^{f/L325R}$; Cdh5-CreERT2$^{+/-}$) mice[20] were made by breeding *Tln1*$^{f/L325R}$[20] with the EC-specific Cdh5-CreERT2 mouse line [27,26]. Studies using the tdTomato reporter were done by comparing mice with genotype *Tln1*$^{f/wt}$;Cdh5-CreERT2$^{+/-}$;Rosa26-tdTomato$^{+/-}$ with *Tln1*$^{f/L325R}$;Cdh5-CreERT2$^{+/-}$;Rosa26-tdTomato$^{+/-}$ mice. Similar ratios of males and female mice were used for experiments and experimenters were blinded to the genotypes of mice until all data was collected. In control experiments to test the effects of tamoxifen versus corn oil on survival, mice were randomly assigned to treatment groups. Experimental procedures were approved by the Emory University Institutional Animal Care and Use Committee (IACUC).

Retinal angiogenesis model and staining

Retinal mounts and immunofluorescence were performed as previously described[28]. Briefly, retinas were dissected out of mice at specified times after tamoxifen treatment, fixed in 4% PFA for either 2hrs at Room Temperature or overnight at 4° C. Whole mount retinas were then subject to antibody staining of FITC-lectin staining as previously described[24]. Tissue was mounted using Fluoromount (Life Technologies) and imaging was performed on an Olympus FV1000 inverted confocal microscope. For staining of whole retinal mounts, the vasculature was visualized with FITC-conjugated Isolectin (Vector Labs: FL-1101-5). Where noted, tdTomato was visualized to analyze recombination efficiency across whole retinal mounts. Primary antibodies used for staining were rat anti-mouse CD31 at 1:100 (BD Pharm: 553370), rabbit anti-mouse talin at 1:100 (Santa Cruz: sc-15336) and rabbit anti-mouse collagen IV at 1:100 (Bio-Rad: 21501470). Species specific secondary donkey antibodies conjugated with Alexa-488/568/647 fluorophores at 1:400 (Life Technologies) antibodies were used for primary antibody detection.

Tumor studies

Both LLC and B16-F0 murine tumor models were performed on 8-10 week-old adult Tln1 Het and Tln1 L325R mice which were administered tamoxifen as described above prior to subcutaneous implantation. For B16-F0 experiments, mice were anesthetized by isoflurane in a procedure approved by Emory IACUC two weeks after the last dose of tamoxifen and injected subcutaneously with 5.0 x 10^5 B16-F0 cells. Animal health and tumor growth were monitored for 14 days prior to sacrifice and tumor volume was measured using calipers. After 14 days, tumors were excised and weighed for relative analysis. 1.0 x 10^6 LLC cells were subcutaneously injected into the right or left flank and tumor growth monitored for 14 days after which tumors were excised and weighed. Where noted for frozen sectioning experiments, tumors were perfusion fixed with 4% PFA, excised, further fixed overnight at 4°C in 4% PFA and embedded in O.C.T Compound (TissueTek). 10μm sections were cut from processed tissue every 50um for blood vessel immunostaining experiments.

MLEC isolation, cell culture and lentivirus

MLECs were isolated as previously described[24]. Lungs were harvested from 8-10 week old adult mice, minced, and pushed through a 16G needle followed by enzymatic digestion to obtain a single cell suspension. ECs were sorted with magnetic beads conjugated with ICAM2 antibody (eBiosource) and cells transformed using a retrovirus expressing temperature-sensitive large T-antigen. The floxed talin1 allele was deleted using adenovirus

harboring either GFP (green fluorescence protein)-Cre or GFP alone and then sorted for GFP positivity to generate Tln1 L325R MLECs. MLECs were cultured in DMEM containing 10% fetal bovine serum, 1% penicillin/streptomycin, and 1% glutamine and serum starved for 6 hours prior to cell lysis for western blotting. HUVECs were purchased from Lonza (C-2519A) and were only used below passage 8. HUVECs were cultured in endothelial growth medium (Lonza) and serum starved prior to cell lysis collection. Lentivirus was generated using the pLKO.1 backbone expressing either human talin1 or scramble shRNAs sequences (talin1: 5′- GCCTCAGATAATCTGGTGAAA, scramble: 5′-CGAGGGCGACTTAACCTTAGG). HUVECs were infected for 16-18 hours, puromycin selected 24 hours after infection and 48 hours after infection trypsinized and replated onto fibronectin-coated (Sigma) coverslips.

Western Blotting

Cell lysis was performed in RIPA buffer (150mM NaCl, 50mM Tris pH 7.4, 0.1% SDS, 1% Triton X-100, 1% Sodium deoxycholate, 1mM PMSF, 1mM NaVO4, 1mM NaF, 1mM EDTA, complete protease inhibitor (Roche) and samples clarified by centrifugation at 13,000g for 10 min at 4°C. Protein samples were boiled for 5 minutes in Laemmli buffer containing 10mM DTT and separated on 6% Tris-glyine gels (Invitrogen). Immunoblotting was done using a goat anti-mouse Talin1/2 (Santa Cruz, sc-7534, 1:1000) antibody, anti-pERK1/2 (Cell Signaling, 4370s, 1:500), anti-FAK (Santa Cruz, sc-1688, 1:1000) or β-actin (Sigma, 1:1000). Primary antibody was detected using donkey anti-goat IR680/800 (Thermo, 1:10000), donkey anti-rabbit IR680/800 (Thermo, 1:10000) or donkey anti-mouse IR680/800 (Thermo, 1:10000) with an Odyssey CLx imager (LI-COR).

Immunofluorescence and tissue staining

Tissue sections prepared as described above were subjected to overnight permeabilization and blocking in PBS with 1% BSA and 0.3% Triton-x (PB Buffer) at 4° C. Primary antibody labeling with rat anti-mouse CD31 at 1:100 (BD Pharm: 553370) and goat anti-mouse podocalyxin at 1:100 (R and D Systems: AF1556) were performed in PB Buffer overnight at 4° C followed by PBS+ washes and secondary antibody staining with species specific donkey IgG conjugated with Alexa-488/647 fluorophores at 1:400 (Life Technologies). Imaging was performed on an Olympus FV1000 Confocal Microscope. For edu analysis in neonatal Tln1 CTRL and EC-KO pup retinas, mice were administered 100ug edu 30′ prior to sacrifice, retinal tissue processed as previously described[28] followed by Click-iT detection per manufacturers recommended protocol (Thermo-Fisher: C10340). Retinas were co-stained with FITC-lectin and the # of edu+/FITC-lectin+ cells counted per field of view, β1 integrin activation was measured using the active conformation-specific antibody 9EG7 (BD Biosciences: 553715, 1:100).

Flow Cytometry

Cultured cells were stained in FACs buffer as previously described [24]. Staining was performed on ice using the following antibodies at 1:100 dilutions: CD31 (MEC13.3, Cat # 55373), CD49e (eBioHma5-1, Cat # 12-0493-81), CD49f (eBioGoH3, Cat # 12-0495-81), CD51 (RMV-7, Cat # 12-0512-81, CD61 (2c9.G3, Cat # 12-0611-81), CD29 (Ha2/5, Cat

562153), FC Block (2.4G2, Cat # 553141), AF 647 Isotype Control (RTK2758, Cat # 400526), and PE Isotype Control (eBMG2b, Cat # 12-4732-82).

Image analysis

For vascular area measurements, stitched images were acquired of the entire retinal tissue. The retinal area was measured and the vascular area is representation of FITC-lectin positive areas within the greater retinal area using FIJI analysis. Junctional Density was measured using AngioTool[29] by masking the FITC-lectin positive area within each field of view and then algorithmic fitting of branching points within the thresholded vascular area to determine junctional density per area. This analysis was performed on 4-6 images per retina analyzed with the n>4 for all groups. For sprout and filopodia quantitation, high magnification (60x,100x) images of overnight 4% PFA-fixed whole-mount retinas were analyzed by counting the number of either structure across the length of the angiogenic front from 4-6 images per retina. 4-6 retinas were analyzed per group as noted in the figure legends. Collagen IV+/lectin- sleeves were measured by taking 3-5 images from 3-4 retina per group. Collagen IV+/lectin- were identified using Image J and normalized to the vascular area within each field of view. For tdTomato tumor blood vessel quantitation, 3 frozen sections from 8-9 tumors were analyzed. 3-4 20x images from each frozen section was thresholded using FIJI binary thresholding and values representing %tdTomato+ area per field of view analyzed. To analyze Pod+/Tom+ blood vessels in B16-F0 tumor sections, 4-6 fields of view from 2 individual frozen sections of 5-6 tumors per group were analyzed. Images were thresholded using pre-set FIJI settings across all acquired images and % area of each channel was then measured using FIJI. Ratios represent the % areas of either Pod+ or Tom+ vessels across identical fields of view.

Statistical analysis

All statistical tests were performed and survival curves generated using Prism Software 8.0. The specific test that was used. to analyze individual experiments is noted in the figure legends but briefly for comparison of parametric data from two groups, an unpaired t-test was used. Data sets analyzed with parametric statistical tests were tested for a normal distribution using a Shapiro-Wilk test.

Results

Endothelial cell talin1 is indispensable for postnatal development

To test the role of EC talin1 during postnatal angiogenesis, we generated EC-specific talin1 knockout mice using *Tln1* floxed mice[18,19] expressing a tamoxifen-inducible Cre driven by the cadherin 5 (*Cdh5*) promoter[26]. Our breeding scheme generated $Tln1^{f/f}$;Cdh5-CreERT2$^{-/-}$ (referred to as Tln1 CTRL) and $Tln1^{f/f}$;Cdh5-CreERT2$^{+/-}$ (Tln1 EC-KO) neonates which were administered tamoxifen intragastrically on postnatal days 1-3 to induce Cre-mediated deletion of talin1. To examine talin1 protein levels in Tln1 CTRL and Tln1 EC-KO pups, retinas were excised at P5 and the retinal endothelium immunostained for talin (Fig. 1a). Tln1 EC-KO retinal ECs exhibited a marked reduction in talin1 protein signal relative to Tln1 CTRL. This finding is consistent with our recently published data showing that lung ECs isolated from adult Tln1 EC-KO mice had significantly reduced levels of

talin protein and transcript levels relative Tln1 CTRL lung ECs[24]. Induction of talin deletion during P1-P3 resulted in early lethality of Tln1 EC-KO mice by P8 whereas Tln1 CTRL littermates survive normally (Fig. 1b). To understand the lethality observed in Tln1 EC-KO mice, tamoxifen-injected pups were sacrificed at P5 and whole organs analyzed after sacrifice. Tln1 EC-KO mice exhibited cranial hemorrhaging which were not present in brains excised from Tln1 CTRL mice (Fig. 1c). Additionally, histological sections of small intestine tissue excised from Tln1 EC-KO mice displayed extensive extravascular red blood cell accumulation in the intestinal villi while the intestinal villi of Tln1 CTRL mice appeared intact and normal (Fig 1d). This phenotype was also observed in H and E sections of Tln1 EC-KO brains whereas Tln1 CTRL brain sections appeared normal. Collectively, these data point to the indispensable function of EC talin1 during postnatal development across a number of vascular beds.

EC talin1 is required for retinal angiogenesis and EC proliferation

Previous studies have established the requirement of EC talin1 during embryonic angiogenesis though little is known about the contributions of talin during postnatal angiogenesis. As the retinal vasculature develops postnatally, we utilized the retinal angiogenesis model to test the contributions of EC talin1 during postnatal angiogenesis[28]. Retinas were dissected from Tln1 CTRL and Tln1 EC-KO pups at P5 and the endothelium visualized by FITC-lectin staining. The total FITC-lectin+ vascular areas of Tln1 EC-KO retinas were reduced by 30% relative to Tln1 CTRL littermates (Fig. 2a). Furthermore, Tln1 EC-KO vascular networks appeared underdeveloped as measured by a reduction in the junctional density of the vascularized areas relative to Tln1 CTRL retinas (Fig. 2b). Analysis of the angiogenic front where individual ECs sprout from pre-existing vessels to form a new vessel revealed an approximately 50% reduction in EC sprouts in Tln1 EC-KO retinas relative to littermate controls (Fig. 2c). Although Tln1 EC-KO retinas had fewer sprouts across the angiogenic front, these sprouts exhibited a higher number of filopodia protrusions suggesting that ECs are able to extend filopodial protrusions, but that ECs are then unable to migrate through the ECM (Fig. 2d). We hypothesized that reduced sprout formation and a reduced vascular area throughout the retina in Tln1 EC-KO mice may be suggestive of altered EC proliferation rates in retinal ECs from Tln1 EC-KO retinas relative to control littermates. We assessed EC proliferation in Tln1 CTRL and Tln1 EC-KO retinal vessels through intragastric injection of 5-Ethynyl-2′-deoxyuridine (EdU) prior to excision of the eye. To selectively analyze proliferating ECs, retinas were subject to FITC-lectin staining to visualize only the endothelium. Indeed, the number of lectin+/edu+ cells were significantly reduced in Tln1 EC-KO retinas relative to retinas from Tln1 CTRL pups (Fig. 2e). The reduction in EC proliferation was noted throughout the vascular network at both the angiogenic front as well as in already established vessels within the central plexus of the network. Interestingly, mature vessels of Tln1 EC-KO retinas were significantly smaller than those of Tln1 CTRL retinal veins possibly due to reduced rates of EC proliferation (Fig. 2f). To analyze vascular patterning of the vascular networks of Tln1 CRL and EC-KO retinas, we used AngioTool software (NCI) to measure lacunarity of the retinal vasculature[29]. Tln1 L325R were less regularly spaced indicative of greater avascular area of Tln1 EC-KO retinas relative to Tln1 CTRL (Fig. 2g). To measure the vascular stability of the retinal vessels, we stained for the basement membrane component collagen IV (coll IV) in conjunction with

FITC-lectin staining to measure the number of collagen IV+/lectin- sleeves. The presence of basement membrane without a lectin+ vessel is indicative of vessel retraction which was increased approximately three-fold in Tln1 EC-KO retinas compared to the Tln1 CTRL retinas (Fig. 2h). The observed reductions in EC proliferation, retinal vascularization, EC sprouting and increased instability of Tln1 EC-KO vessels highlight the essential function of EC talin1 during retinal angiogenesis.

Expression of an integrin activation-deficient talin1 L325R inhibits retinal angiogenesis

Talin activates integrins by binding to the β-integrin cytoplasmic tail at two distinct sites to induce the active conformation of the integrin receptor [16,15,30,31]. We and others have reported a single amino acid mutation in the talin head (talin1 L325R) which inhibits the membrane proximal interaction required for talin to activate integrin yet retains binding to the membrane-distal site that mechanically links integrins to actin[32,20] . Induced expression of this mutant in mouse platelets inhibited platelet integrin activation and resulted in impaired platelet function during hemostasis and thrombosis[21]. We hypothesized that expression of talin1 L325R in ECs would allow us to discern the specific requirement of talin-mediated integrin activation from its integrin-independent functions and allow us to specifically test the requirement of inside-out integrin activation during angiogenesis. We generated *Tln1*$^{f/wt}$; Cdh5-CreERT2$^{+/-}$ (referred to as Tln1 Het) and *Tln1*$^{f/L325R}$; Cdh5-CreERT2$^{+/-}$ (Tln1 L325R) mice by crossing previously described *Tln1*$^{f/L325R}$ mice with an inducible EC-specific Cre-recombinase mouse line. As a single allele of *Tln1* is sufficient for normal development and for platelet integrin activation[21], control mice in the experiments done in comparison to Tln1 L325R mice are heterozygous for the *Tln1* allele in order to accommodate breeding in of a tdTomato reporter allele to keep track of genetic recombination. Recombination efficiency of Cre-mediated talin deletion was measured by qualitative analysis of tdTomato reporter expression in retinal vessels and in later experiments, frozen tumor sections (Online Resource I and II). Tln1 Het and Tln1 L325R neonates were intragastrically administered tamoxifen once per day to induce Cre activity from P1 to P3. Intriguingly, Tln1 Het and Tln1 L325R mice both reach weaning age and adulthood, but Tln1 L325R exhibited a marked reduction in body weight and development that was maintained into adulthood (Fig. 3a, 3b). The Tln1 L325R phenotype differed from the early lethality observed in Tln1 EC-KO mice. Curiously, Tln1 L325R retinas examined at P5 exhibited defects in retinal angiogenesis as measured by vascular area and vascular density relative to Tln1 Het control mice (Fig. 3c, 3d). Furthermore, vascular networks of Tln1 L325R retinas were less regularly spaced as measured by lacunarity analysis relative to their littermate controls (Fig 3e). Additionally, Tln1 L325R retinal vessels exhibited reduced levels of active β1 integrin activation relative to littermate controls (Online Resource V). These collective data indicate a requirement of talin-mediated EC integrin activation during retinal angiogenesis but also point to other possible talin-dependent functions that may be required for postnatal development given the severity of the phenotype observed in Tln1 EC-KO mice.

Inhibition of integrin activation dysregulates EC MAPK-ERK signaling

Given the observed reductions in vascular growth in Tln1 EC-KO and Tln1 L325R retinas, we speculated whether altered MAPK signaling, an essential pro-growth pathway, may

explain these defects. Previous studies in other cell types have supported the notion that loss of integrin activation, either due to deletion of talin1 [33] or kindlin-3[34] promotes aberrant MAPK signaling as measured by phosphorylation of ERK1/2. In light of a recent study from Pontes-Quero and colleagues[35] describing the negative regulatory mechanism by which abnormal increases in EC mitogenic signaling induces EC cell-cycle arrest causing impaired retinal angiogenesis, we sought to measure MAPK signaling in talin1-depleted and talin1 L325R-expressing ECs. We utilized lentiviral short hairpin RNA (shRNA) constructs to delete talin1 in cultured human umbilical vein ECs (HUVECs) and measured basal p-ERK1/2 levels. Indeed, serum-starved shTln1 HUVECs exhibited marked increases in p-ERK1/2 status relative to shScramble controls indicating that deletion of talin1 is associated with altered MAPK signaling (Fig. 4a). To determine whether aberrant p-ERK1/2 levels were due to loss of integrin activation or integrin-independent roles of talin1, we measured assessed MAPK signaling in mouse lung endothelial cells (MLECs) isolated from Tln1 Het and Tln1 L325R mouse lungs. Tln1 Het and Tln1 L325R MLEC surface integrin expression levels of α5, α6 αv, β1 and β3-subunits were similar between groups (Online Resource III). Basal levels of p-ERK1/2 in Tln1 L325R MLECs were significantly increased relative to Tln1 Het control MLECs (Fig. 4b) suggesting that impaired integrin activation is likely responsible for the increase in p-ERK1/2 levels. These collective data suggest a novel interplay linking integrin activation with regulation of MAPK signaling that may be in part responsible for the observed defects in postnatal angiogenesis.

EC integrin activation is indispensable for tumor angiogenesis and lumen formation

Given the observed defects in retinal angiogenesis exhibited in Tln1 L325R pups, we wondered whether talin-dependent integrin activation played a similar role in pathological contexts of angiogenesis in these mice. To answer this question, we subcutaneously injected B16-F0 murine melanoma cells and analyzed the growth of primary tumors as well as the vascularization of the tumors in Tln1 Het and L325R adult mice 2-weeks after tamoxifen-mediated activation of Cre-recombinase. Strikingly, tumors injected in Tln1 L325R mice grew slower than Tln1 Het tumors and were 55% smaller by weight at removal 14 days post-implantation (Fig. 5a). These tumors were excised, processed for frozen sectioning and blood vessel density of tumors in both groups analyzed. Tln1 L325R frozen sections had an approximately 50% reduction in tdTomato+ area relative to Tln1 Het tumor sections (Fig. 5b). Given the significant reduction in blood vessel density in Tln1 L325R tumors and the well-established paradigm that tumor vessels are immature, we wondered whether the vessels in the respective tumor groups differed in the extent of their lumenization as measured by the luminal marker Podocalyxin (Pod). To test this question, we stained Tln1 Het and L325R B16-F0 tumor sections and quantitated the coverage of Pod+Tom+/Pod+ and Pod+Tom+/Tom+ events. The first metric represents the proportion of lumenized, recombined vessels to all lumenized vessels in the section while the second metric represents the ratio of lumenized, recombined vessels to all recombined vessels. Tln1 Het and L325R tumors contained a similar number of Pod+Tom+/Tom+ vessels whereas Tln1 L325R contained fewer Pod+Tom+/Pod+ structures meaning a number of the vessels in L325R tumors were likely unrecombined, lumenized structures and thus wildtype talin1 containing vessels (Fig. 5c). We concluded that expression of wildtype talin1 is necessary for vessel lumenization and that the absence of integrin activation in Talin1 L325R

tumor ECs likely results in a growth disadvantage. We used an independent syngeneic lung cancer cell line, Lewis Lung Carcinoma (LLC), to test whether the defects in tumor growth observed with B16-F0 were applicable to other primary tumor models. LLC tumors grown in Tln1 L325R mice were 31% smaller by mass relative to those grown Tln1 Het mice although this data did not reach statistical significance (p-value = 0.0562) (Fig. 5d). Curiously, the necrotic area of Tln1 L325R tumors was reduced relative to Tln1 CTRL B16-F0 tumors suggesting that diminished tumor angiogenesis correlates with reduces tumor necrosis (Fig. 5e and Online Resource IV). Together, these data indicate that expression of talin1 L325R strongly inhibits tumor angiogenesis in a cell-autonomous fashion suggesting that EC integrin activation is essential for pathological blood vessel growth.

Discussion

Our results provide the first evidence that endothelial cell integrin activation is requisite for retinal and pathological angiogenesis. To test the requirement of integrin activation in these contexts, we utilized two novel mouse models: 1) an inducible, EC-specific talin1 knockout model 2) an inducible, EC-specific talin1 L325R model in which talin can bind to, but not activate, integrins. Induced deletion of EC-talin1 in neonates resulted in early lethality of Tln1 EC-KO pups by P8. Tln1 EC-KO mice exhibited impaired retinal angiogenesis, cranial and gastrointestinal hemorrhaging none of which were observed in control littermates. Deletion of talin1 in retinal endothelium resulted in reduced vascularized area, reduced EC sprouting and reduced EC proliferation relative to retinal vessels of Tln1 CTRL mice. Induction of talin1 L325R expression during early postnatal development resulted in smaller mice at weaning age relative to control littermates and these lower body weights persisted into adulthood. Notably, we did not observe reduced survival in Tln1 L325R as we observed in Tln1 EC-KO pups. Tln1 L325R neonates exhibited impaired retinal angiogenesis as measured by vascular area and vascular density relative to their Tln1 Het littermates. We observed increased MAPK signaling in both talin1-depleted and talin1 L325R ECs suggesting that loss of integrin activation adversely dysregulated MAPK signaling. Strikingly, Tln1 L325R adult mice subcutaneously implanted with either B16-F0 murine melanoma or Lewis Lung Carcinoma grew smaller tumors than their control counterparts with defects in tumor vascularization. Together these data indicate that talin-mediated integrin activation is required during postnatal angiogenesis and also highlight the intriguing finding that integrin-independent functions of talin may play a critical, not yet fully understood role in new blood vessel growth.

An important consideration in light of the observed differences between the Tln1 EC-KO and Tln1 L325R neonates is that ablation of talin eliminates an important adaptor protein that mechanically links integrin to the actin cytoskeleton[36,37]. Presumably, Talin1 L325R retains this actin cytoskeleton linkage capacity in ECs. Indeed, the importance of the linkage to the actin cytoskeleton is highlighted in the different phenotypes observed in talin1 L325R and talin1-null platelets during clot retraction[20]. Whereas both talin1 L325R and talin1-null platelets exhibit defects in clot retraction, a process which requires integrin to be linked to the actin cytoskeleton, defects in talin1 L325R platelet clot retraction could be rescued by exogenously activating integrins with manganese but were lost when actin polymerization was inhibited by cytochalasin D[21]. Importantly, reports from Stefanini

and colleagues as well as Haling and colleagues both report indicate that there is no difference in binding affinity of the L325R mutant relative to wildtype talin1[20,21]. This observation indicates that the integrin-talin(L325R)-actin cytoskeleton linkage remains functionally intact. Therefore, it is reasonable to extrapolate that differences in Tln1 EC-KO and Tln1 L325R pup development may be due to retention of the talin rod interactions with the actin cytoskeleton in L325R pups. Additionally, the absence of the talin rod disrupts mechanosensitive interactions of the talin with the actin binding protein vinculin which binds cryptic sites in the talin rod that are exposed in tension-dependent manner [38,36]. Specific vinculin-talin interactions promote binding of talin to actin cytoskeleton and are indispensable for focal adhesion stability[39]. Therefore, it is possible that talin engagement with the acto-myosin machinery may be of importance in other vascular beds other than the retina such as the small intestine and the brain where hemorrhaging was observed in Tln1 EC-KO pups (Fig. 1c, 1d) but absent in Tln1 L325R pups. It is plausible that ECs in these vascular beds are subject to increased mechanical forces which in the absence of talin result in vascular instability but are mitigated in the presence of talin1 L325R.

As deletion of EC talin1 in established vessels is lethal due to defects in vascular permeability that are in part regulated by β1 integrin activation[24], it is remarkable that induction of talin1 L325R in already established vessels does not result in a similar effect on quiescent vessels. The aforementioned talin rod-mediated interactions with the actin-cytoskeleton may also explain the disparity in these two models meaning there are likely other important functions of talin outside of its role in activating integrins that may be of note in mature vasculature. However, while mature vessels in quiescent states appear unaffected by talin1 L325R induction (data not shown), Tln1 L325R mice display extensive defects in tumor growth and angiogenesis relative to their littermate controls suggesting that the defects observed in tumor angiogenesis in Tln1 L325R mice are due to defective integrin activation. Furthermore, the observation that the number of unrecombined, lumenized vessels were increased 39% in Tln1 L325R B16-F0 tumors indicates that Tln1 L325R may be critical in the process by which immature vessels, stabilize and form lumens. This result is suggestive of integrin-activation-independent interactions of talin with other proteins that may be critical for lumen formation and is reminiscent of a report from Zovein and colleagues wherein deletion of β1 integrin in ECs during development resulted in occluded, unlumenized vessels[40] due to deficient Par3-mediated EC polarization during developmental angiogenesis. It may therefore be prudent to investigate the contributions of talin1 to EC polarity and whether talin1-null ECs exhibit altered Par3 signaling.

Though differences were observed in the postnatal angiogenesis and survival phenotype between Tln1 EC-KO and Tln1 L325R pups, there were several commonalities amongst the models that warrant further investigation. As deletion of talin1 and expression of the talin1 L325R mutant impairs EC integrin activation, we predicted that there would be comparable defects in postnatal angiogenesis given previous studies establishing the requirement of EC talin1 for embryonic angiogenesis. Indeed, both Tln1 EC-KO and Tln1 L325R retinas exhibited marked reductions in retinal vascularization and vascular density relative to their respective littermate controls (Fig. 2a, 2b, 3c and 3d). Defects in tumor angiogenesis were also observed in Tln1 L325R adult mice indicating that pathological angiogenesis was also affected (Fig. 5b). Furthermore, tln1-deficient and ECs isolated from Tln1 L325R lungs

exhibited significant upregulation of MAPK signaling as measured by p-ERK1/2 levels (Fig. 4). It is therefore reasonable to conclude that in the absence of integrin activation during angiogenesis, MAPK signaling becomes dysregulated and may partially explain defects in new vessel growth. This conclusion agrees with the Pontes-Quero et al. study[35] wherein heightened mitogenic signaling impairs angiogenesis by inducing cell-cycle arrest. However, it will be prudent to investigate the underlying mechanism through which integrin activation appears to negatively regulate MAPK signaling. Additionally, are defects observed in vessel growth and lumen formation in Tln1 L325R tumors driven by defects in integrin signaling of a specific heterodimer or subunit? Can the observed differences be “rescued” through exogenous activation of integrins? Collectively, our studies point to a role for EC talin1 during postnatal angiogenesis at least in part through its integrin activating function. Future investigation into the molecular mechanisms underlying our observed defects in postnatal and tumor angiogenesis in Tln1 L325R mice should be enlightening.

Supplementary Material

Refer to Web version on PubMed Central for supplementary material.

Acknowledgements:

We thank the following investigators for generously providing mice used in these studies: David Critchley and Susan Monkley (Tln1fl/fl mice) and Ralf Adams (Cdh5-CreERT2 mice). We are also grateful for support from Children’s Healthcare of Atlanta and the Emory University Integrated Cellular Imaging Core.

Sources of Funding:

This work was supported in part by National Institutes of Health National Heart, Lung, and Blood Institute grant HL117061 (B.G. Petrich), HL098435, HL133497, HL141155 (A.W. Orr), F31HL136194 (F.E. Pulous), Emory University School of Medicine Bridge Funding Grant 00098174, the Winship Invest$ Pilot Grant 00099018, Aflac Pilot Grant 00080676, Mark Foundation for Cancer Research Grant 18-031-ASP (C.J. Henry), and ASH Minority Hematology Graduate Award 0000055928 (J. A. G. Hamilton).

References

1. Bergers G, Benjamin LE (2003) Tumorigenesis and the angiogenic switch. Nat Rev Cancer 3 (6):401–410. doi:10.1038/nrc1093 [PubMed: 12778130]
2. Potente M, Gerhardt H, Carmeliet P (2011) Basic and therapeutic aspects of angiogenesis. Cell 146 (6):873–887. doi:10.1016/j.cell.2011.08.039 [PubMed: 21925313]
3. Carmeliet P, Jain RK (2011) Molecular mechanisms and clinical applications of angiogenesis. Nature 473 (7347):298–307. doi:10.1038/nature10144 [PubMed: 21593862]
4. Hynes RO, Lively JC, McCarty JH, Taverna D, Francis SE, Hodivala-Dilke K, Xiao Q (2002) The diverse roles of integrins and their ligands in angiogenesis. Cold Spring Harb Symp Quant Biol 67:143–153 [PubMed: 12858535]
5. Hynes RO (2002) Integrins: bidirectional, allosteric signaling machines. Cell 110 (6):673–687 [PubMed: 12297042]
6. Stupack DG, Cheresh DA (2002) ECM remodeling regulates angiogenesis: endothelial integrins look for new ligands. Sci STKE 2002 (119):pe7. doi:10.1126/stke.2002.119.pe7 [PubMed: 11842241]
7. Foubert P, Varner JA (2012) Integrins in tumor angiogenesis and lymphangiogenesis. Methods Mol Biol 757:471–486. doi:10.1007/978-1-61779-166-6_27 [PubMed: 21909928]
8. Bledzka K, Bialkowska K, Sossey-Alaoui K, Vaynberg J, Pluskota E, Qin J, Plow EF (2016) Kindlin-2 directly binds actin and regulates integrin outside-in signaling. J Cell Biol 213 (1):97–108. doi:10.1083/jcb.201501006 [PubMed: 27044892]

9. Law DA, Nannizzi-Alaimo L, Phillips DR (1996) Outside-in integrin signal transduction. Alpha IIb beta 3-(GP IIb IIIa) tyrosine phosphorylation induced by platelet aggregation. J Biol Chem 271 (18):10811–10815 [PubMed: 8631894]
10. Mahabeleshwar GH, Feng W, Reddy K, Plow EF, Byzova TV (2007) Mechanisms of integrin-vascular endothelial growth factor receptor cross-activation in angiogenesis. Circ Res 101 (6):570–580. doi:10.1161/CIRCRESAHA.107.155655 [PubMed: 17641225]
11. De S, Razorenova O, McCabe NP, O'Toole T, Qin J, Byzova TV (2005) VEGF-integrin interplay controls tumor growth and vascularization. Proc Natl Acad Sci U S A 102 (21):7589–7594. doi:10.1073/pnas.0502935102 [PubMed: 15897451]
12. Mahabeleshwar GH, Feng W, Phillips DR, Byzova TV (2006) Integrin signaling is critical for pathological angiogenesis. J Exp Med 203 (11):2495–2507. doi:10.1084/jem.20060807 [PubMed: 17030947]
13. Sahni A, Khorana AA, Baggs RB, Peng H, Francis CW (2006) FGF-2 binding to fibrin(ogen) is required for augmented angiogenesis. Blood 107 (1):126–131. doi:10.1182/blood-2005-06-2460 [PubMed: 16160009]
14. Yang L, O'Neill P, Martin K, Maass JC, Vassilev V, Ladher R, Groves AK (2013) Analysis of FGF-dependent and FGF-independent pathways in otic placode induction. PLoS One 8 (1):e55011. doi:10.1371/journal.pone.0055011 [PubMed: 23355906]
15. Tadokoro S, Shattil SJ, Eto K, Tai V, Liddington RC, de Pereda JM, Ginsberg MH, Calderwood DA (2003) Talin binding to integrin beta tails: a final common step in integrin activation. Science 302 (5642):103–106. doi:10.1126/science.1086652 [PubMed: 14526080]
16. Calderwood DA, Zent R, Grant R, Rees DJ, Hynes RO, Ginsberg MH (1999) The Talin head domain binds to integrin beta subunit cytoplasmic tails and regulates integrin activation. J Biol Chem 274 (40):28071–28074 [PubMed: 10497155]
17. Shattil SJ, Kim C, Ginsberg MH (2010) The final steps of integrin activation: the end game. Nat Rev Mol Cell Biol 11 (4):288–300. doi:10.1038/nrm2871 [PubMed: 20308986]
18. Petrich BG, Marchese P, Ruggeri ZM, Spiess S, Weichert RA, Ye F, Tiedt R, Skoda RC, Monkley SJ, Critchley DR, Ginsberg MH (2007) Talin is required for integrin-mediated platelet function in hemostasis and thrombosis. J Exp Med 204 (13):3103–3111. doi:10.1084/jem.20071800 [PubMed: 18086863]
19. Nieswandt B, Moser M, Pleines I, Varga-Szabo D, Monkley S, Critchley D, Fassler R (2007) Loss of talin1 in platelets abrogates integrin activation, platelet aggregation, and thrombus formation in vitro and in vivo. J Exp Med 204 (13):3113–3118. doi:10.1084/jem.20071827 [PubMed: 18086864]
20. Haling JR, Monkley SJ, Critchley DR, Petrich BG (2011) Talin-dependent integrin activation is required for fibrin clot retraction by platelets. Blood 117 (5):1719–1722. doi:10.1182/blood-2010-09-305433 [PubMed: 20971947]
21. Stefanini L, Ye F, Snider AK, Sarabakhsh K, Piatt R, Paul DS, Bergmeier W, Petrich BG (2014) A talin mutant that impairs talin-integrin binding in platelets decelerates alphaIIbbeta3 activation without pathological bleeding. Blood 123 (17):2722–2731. doi:10.1182/blood-2013-12-543363 [PubMed: 24585775]
22. Avraamides CJ, Garmy-Susini B, Varner JA (2008) Integrins in angiogenesis and lymphangiogenesis. Nat Rev Cancer 8 (8):604–617. doi:10.1038/nrc2353 [PubMed: 18497750]
23. Monkley SJ, Kostourou V, Spence L, Petrich B, Coleman S, Ginsberg MH, Pritchard CA, Critchley DR (2011) Endothelial cell talin1 is essential for embryonic angiogenesis. Dev Biol 349 (2):494–502. doi:10.1016/j.ydbio.2010.11.010 [PubMed: 21081121]
24. Pulous FE, Grimsley-Myers CM, Kansal S, Kowalczyk AP, Petrich BG (2019) Talin-Dependent Integrin Activation Regulates VE-Cadherin Localization and Endothelial Cell Barrier Function. Circ Res 124 (6):891–903. doi:10.1161/CIRCRESAHA.118.314560 [PubMed: 30707047]
25. Pulous FE, Petrich BG (2019) Integrin-dependent regulation of the endothelial barrier. Tissue Barriers:1685844. doi:10.1080/21688370.2019.1685844 [PubMed: 31690180]
26. Wang Y, Nakayama M, Pitulescu ME, Schmidt TS, Bochenek ML, Sakakibara A, Adams S, Davy A, Deutsch U, Luthi U, Barberis A, Benjamin LE, Makinen T, Nobes CD, Adams RH (2010)

Ephrin-B2 controls VEGF-induced angiogenesis and lymphangiogenesis. Nature 465 (7297):483–486. doi:10.1038/nature09002 [PubMed: 20445537]

27. Monvoisin A, Alva JA, Hofmann JJ, Zovein AC, Lane TF, Iruela-Arispe ML (2006) VE-cadherin-CreERT2 transgenic mouse: a model for inducible recombination in the endothelium. Dev Dyn 235 (12):3413–3422. doi:10.1002/dvdy.20982 [PubMed: 17072878]
28. Pitulescu ME, Schmidt I, Benedito R, Adams RH (2010) Inducible gene targeting in the neonatal vasculature and analysis of retinal angiogenesis in mice. Nat Protoc 5 (9):1518–1534. doi:10.1038/nprot.2010.113 [PubMed: 20725067]
29. Zudaire E, Gambardella L, Kurcz C, Vermeren S (2011) A computational tool for quantitative analysis of vascular networks. PLoS One 6 (11):e27385. doi:10.1371/journal.pone.0027385 [PubMed: 22110636]
30. Wegener KL, Partridge AW, Han J, Pickford AR, Liddington RC, Ginsberg MH, Campbell ID (2007) Structural basis of integrin activation by talin. Cell 128 (1):171–182. doi:10.1016/j.cell.2006.10.048 [PubMed: 17218263]
31. Anthis NJ, Haling JR, Oxley CL, Memo M, Wegener KL, Lim CJ, Ginsberg MH, Campbell ID (2009) Beta integrin tyrosine phosphorylation is a conserved mechanism for regulating talin-induced integrin activation. J Biol Chem 284 (52):36700–36710. doi:10.1074/jbc.M109.061275 [PubMed: 19843520]
32. Kopp PM, Bate N, Hansen TM, Brindle NP, Praekelt U, Debrand E, Coleman S, Mazzeo D, Goult BT, Gingras AR, Pritchard CA, Critchley DR, Monkley SJ (2010) Studies on the morphology and spreading of human endothelial cells define key inter- and intramolecular interactions for talin1. Eur J Cell Biol 89 (9):661–673. doi:10.1016/j.ejcb.2010.05.003 [PubMed: 20605055]
33. Chen P, Lei L, Wang J, Zou X, Zhang D, Deng L, Wu D (2017) Downregulation of Talin1 promotes hepatocellular carcinoma progression through activation of the ERK1/2 pathway. Cancer Sci 108 (6):1157–1168. doi:10.1111/cas.13247 [PubMed: 28375585]
34. Dudiki T, Meller J, Mahajan G, Liu H, Zhevlakova I, Stefl S, Witherow C, Podrez E, Kothapalli CR, Byzova TV (2020) Microglia control vascular architecture via a TGFbeta1 dependent paracrine mechanism linked to tissue mechanics. Nat Commun 11 (1):986. doi:10.1038/s41467-020-14787-y [PubMed: 32080187]
35. Pontes-Quero S, Fernandez-Chacon M, Luo W, Lunella FF, Casquero-Garcia V, Garcia-Gonzalez I, Hermoso A, Rocha SF, Bansal M, Benedito R (2019) High mitogenic stimulation arrests angiogenesis. Nat Commun 10 (1):2016. doi:10.1038/s41467-019-09875-7 [PubMed: 31043605]
36. Gingras AR, Bate N, Goult BT, Patel B, Kopp PM, Emsley J, Barsukov IL, Roberts GC, Critchley DR (2010) Central region of talin has a unique fold that binds vinculin and actin. J Biol Chem 285 (38):29577–29587. doi:10.1074/jbc.M109.095455 [PubMed: 20610383]
37. Gingras AR, Bate N, Goult BT, Hazelwood L, Canestrelli I, Grossmann JG, Liu H, Putz NS, Roberts GC, Volkmann N, Hanein D, Barsukov IL, Critchley DR (2008) The structure of the C-terminal actin-binding domain of talin. EMBO J 27 (2):458–469. doi:10.1038/sj.emboj.7601965 [PubMed: 18157087]
38. Yao M, Goult BT, Klapholz B, Hu X, Toseland CP, Guo Y, Cong P, Sheetz MP, Yan J (2016) The mechanical response of talin. Nat Commun 7:11966. doi:10.1038/ncomms11966 [PubMed: 27384267]
39. Atherton P, Stutchbury B, Wang DY, Jethwa D, Tsang R, Meiler-Rodriguez E, Wang P, Bate N, Zent R, Barsukov IL, Goult BT, Critchley DR, Ballestrem C (2015) Vinculin controls talin engagement with the actomyosin machinery. Nat Commun 6:10038. doi:10.1038/ncomms10038 [PubMed: 26634421]
40. Zovein AC, Luque A, Turlo KA, Hofmann JJ, Yee KM, Becker MS, Fassler R, Mellman I, Lane TF, Iruela-Arispe ML (2010) Beta1 integrin establishes endothelial cell polarity and arteriolar lumen formation via a Par3-dependent mechanism. Dev Cell 18 (1):39–51. doi:10.1016/j.devcel.2009.12.006 [PubMed: 20152176]

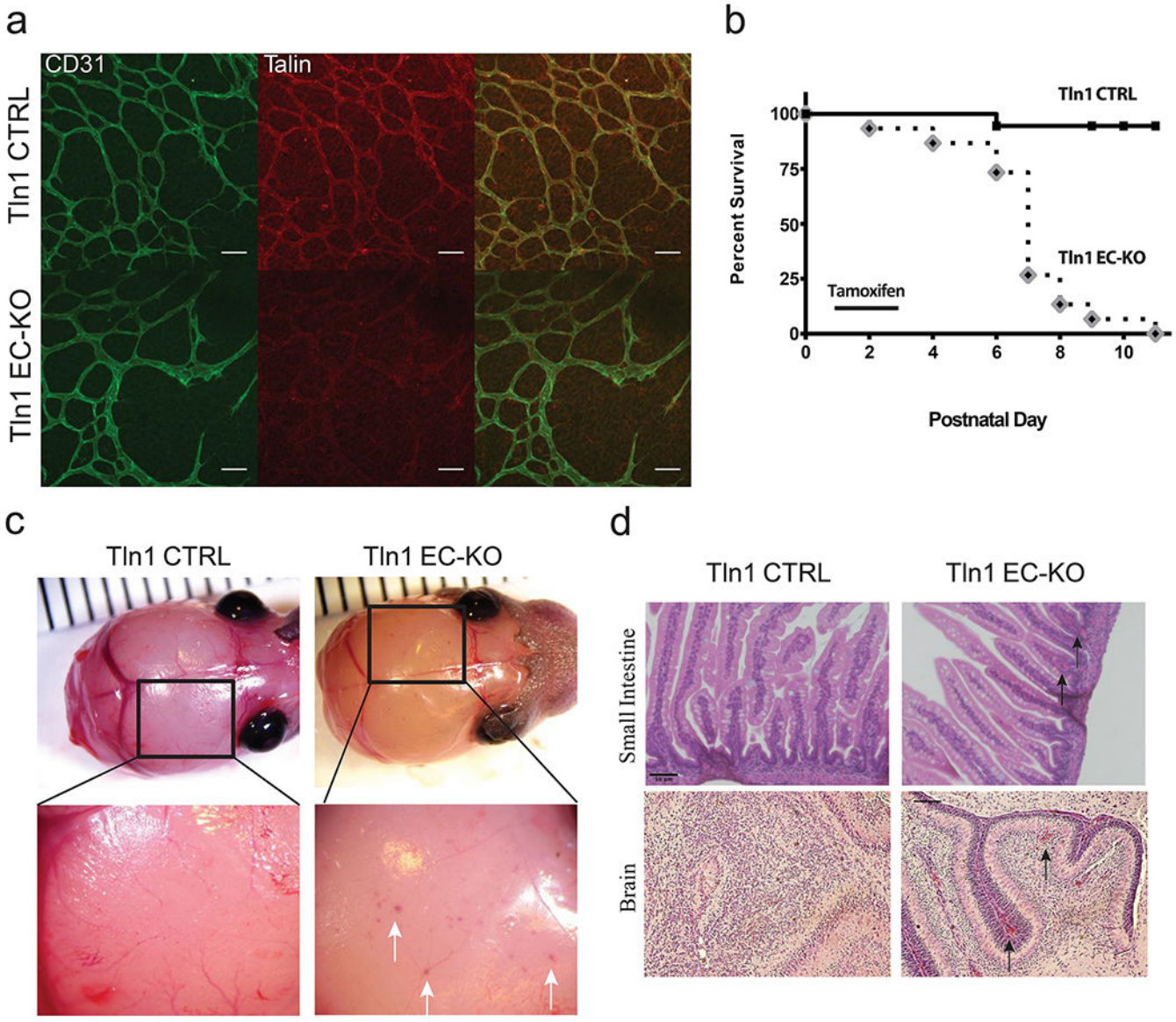

Fig. 1. EC-specific deletion of talin1 during postnatal development causes vascular hemorrhage and death

Tln1 (talin1) EC-KO (knockout;Tln1fl/fl;Cdh5creERT2+/−) and Tln1 CTRL (control; Tln1fl/fl;Cdh5creERT2−/−) neonates were administered tamoxifen P1-P3 and analyzed at P5 where indicated. **(a)** Immunostaining of whole-mounted retinas from Tln1 CTRL and Tln1 EC-KO mice. Talin protein is markedly reduced in Tln1 EC-KO CD31+ECs. (scale= 50 μm) **(b)** Survival of Tln1 EC-KO and Tln1 CTRL mice following tamoxifen treatment. Tln1 EC (n=15, Tln1 CTRL and n=18, Tln1 EC-KO). **(c)** Light microscopy of whole brains from Tln1 CTRL and Tln1 EC-KO mice. Inset zoom highlight focal hemorrhaging (arrows) in brain microvasculature of Tln1 EC-KO pups not observed in Tln1 CTRL mice. **(d)** H and E sections of Tln1 CTRL and EC-KO small intestine and brain from P7 pups. Red blood cell accumulation is observed in Tln1 EC-KO intestinal villi and brain microvessels (arrows) that

is not observed in Tln1 CTRL sections (n=3-5 per group unless otherwise noted, scale = 50 μm)

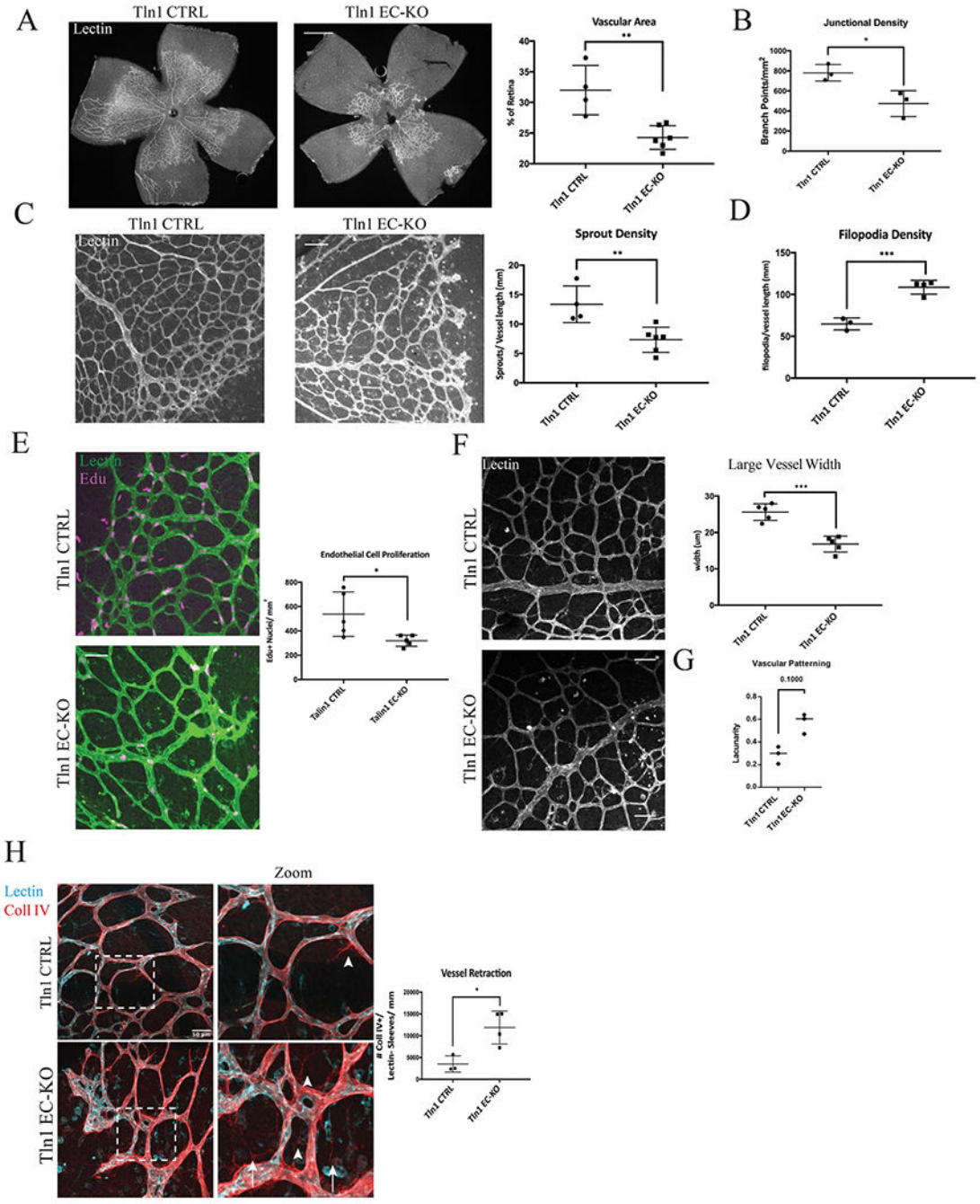

Fig. 2. EC talin1 is required for retinal angiogenesis and EC proliferation

(a) FITC-lectin staining of whole-mount Tln1 CTRL and EC-KO retinas. FITC-lectin+ area was measured as a % of the total retinal area. (scale = 1 mm; **p=.0033) **(b)** Junctional density of Tln1 CTRL and EC-KO retinal vessels visualized by FITC-lectin staining. Retinal vessel area and junction counts were measured using Angiotool and revealed a reduction of vessel junctions in Tln1 EC-KO retinas relative to CTRL (*p= .025) **(c)** Sprout density of Tln1 CTRL and Tln1 EC-KO whole-mount retinas stained with FITC-lectin. The number of sprouts across the length of the angiogenic front were reduced in Tln1 EC-KO retinas

relative to Tln1 CTRL (scale = 100 μm; **p=.0063) **(d)** Filopodia density of Tln1 CTRL and Tln1 EC-KO retinal vessels which were stained with FITC-lectin. The number of filopodia across the length of the angiogenic front were increased in Tln1 EC-KO retinas relative to Tln1 CTRL (n=3-4; ***p=.0007) **(e)** EC proliferation in Tln1 CTRL and Tln1 EC-KO retinal vessels was measured by quantitating edu+/lectin+ events. EC proliferation is reduced in Tln1 EC-KO retinas relative to control littermates (n=4; scale = 50 μm; *p=.045) **(f)** Large vessel widths measured measured in Tln1 CTRL and Tln1 EC-KO retinas stained with FITC-lectin. Large vessel width is reduced in Tln1 EC-KO retinal vasculature relative to Tln1 CTRL (n=5; scale = 50 μm; ***p=.0003) **(g)** Vascular patterning was assessed by automated analysis of lacunarity using AngioTool[29] of Tln1 CTRL and EC-KO P7 retinas. Increased lacunarity of Tln1 EC-KO networks relative to littermate controls indicates increased avascular space between adjacent vessels. (n=3; p=.10; Mann-Whitney Test) **(h)** Vessel retraction in Tln1 CTRL and Tln1 EC-KO retinal vessels measured by staining for basement membrane component Collagen IV (red) in conjunction with FITC-lectin. Retracted vessels are marked by white arrows representing coll IV deposition lacking a new vessel sprout. Vessel retraction is increased in Tln1 EC-KO retinas relative to Tln1 CTRL (n=3-4; scale = 50 μm; *p=.018) (P-values listed for individual experiments were generated using a 2-tailed unpaired t-test, n=3-6 per group unless otherwise noted)

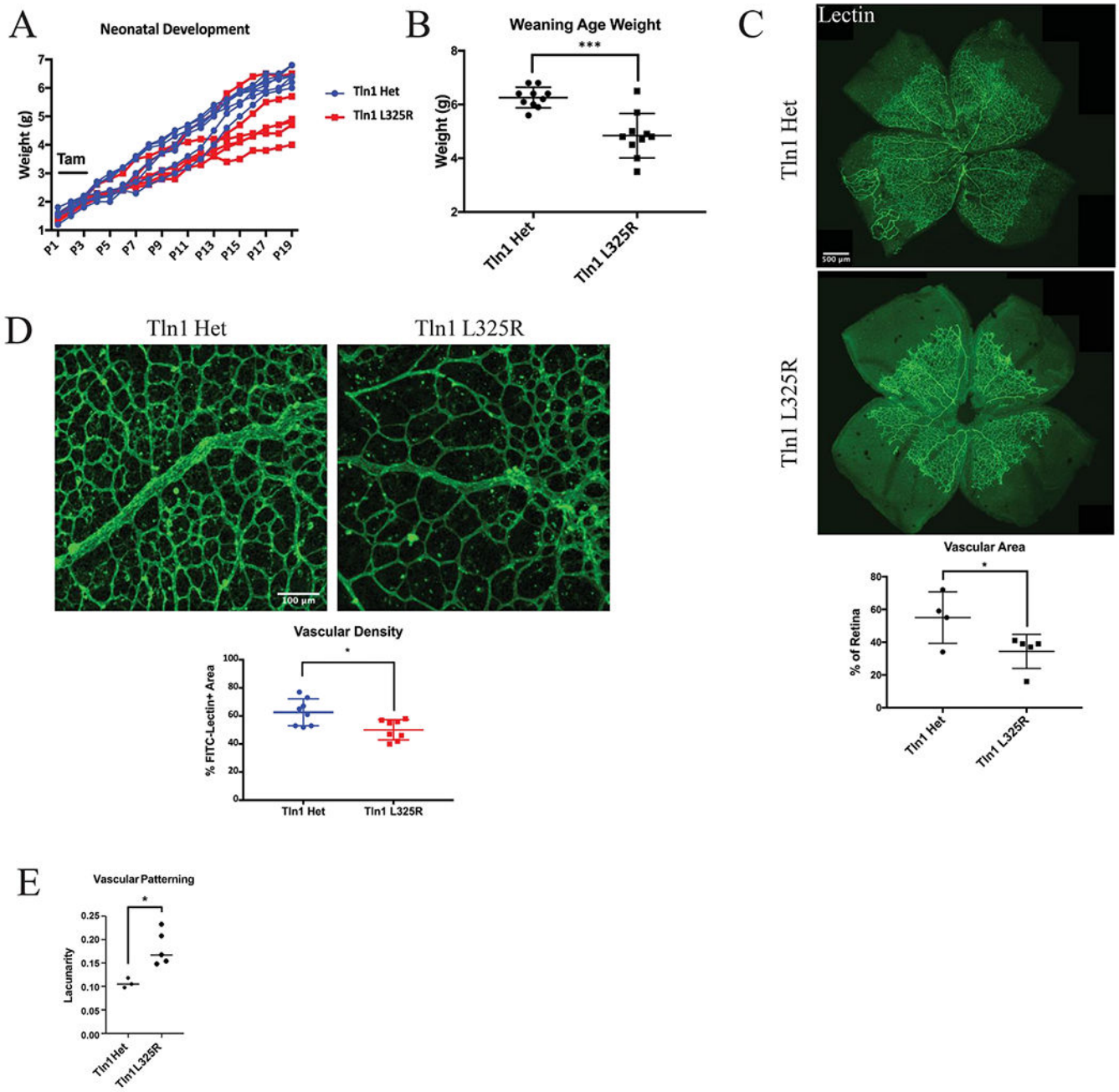

Fig. 3. Expression of an integrin activation-deficient talin1 L325R mutant inhibits retinal angiogenesis

(a) Tln1 Het and Tln1 L325R neonates were weighed daily from P1-P19 prior to weaning. Tln1 L325R pups were undersized relative to littermate control Tln1 Het pups. (n= 7 Tln1 Het and 6 Tln1 L325R) **(b)** Tln1 Het and Tln1 L325R pups were weighed at P24 to determine weaning age weights. Tln1 L325R were 23% smaller than littermate controls. (n=10 per group; *p=.0001) **(c)** Vascular area as % of total retinal area was measured on retinas from P5 Tln1 Het and Tln1 L325R pups stained for FITC-lectin. Total vascularized area was reduced in Tln1 L325R retinas relative to Tln1 Het mice. (n=4-5, scale = 500

μm; *p=.0498) **(d)** Vascular density in P7 Tln1 Het and L325R retinas was measured by staining for FITC-lectin. Tln1 L325R retinas exhibit a less dense vascular network relative to Tln1 Het littermate controls. (n=8; scale = 100 μm; *p=.0105) **(e)** Vascular patterning was assessed by automated analysis of lacunarity using AngioTool [29] of Tln1 Het and L325R P7 retinas. Increased lacunarity of Tln1 L325R networks relative to littermate controls indicates increased avascular space between adjacent vessels. (n=3-5/group; *p=.0356; Mann-Whitney Test) (P-values listed for individual experiments were generated using a 2-tailed unpaired t-test).

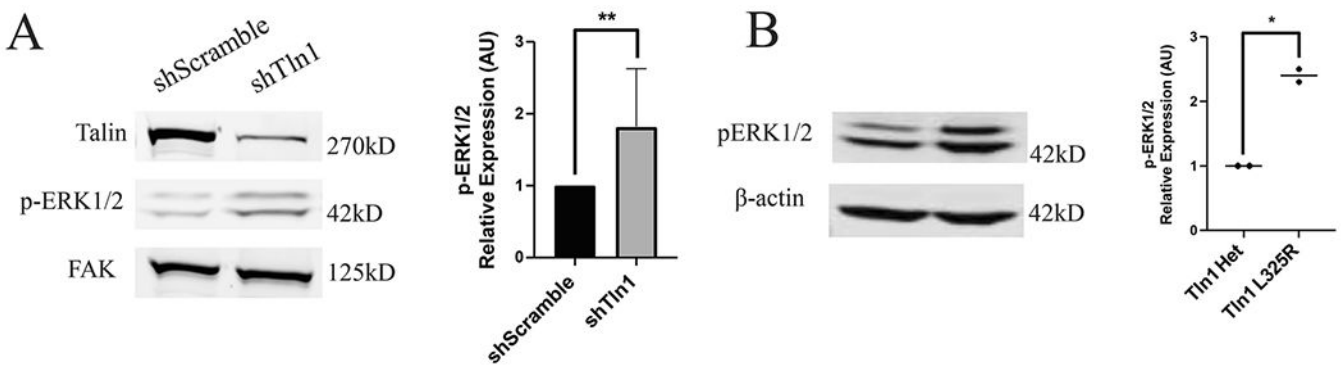

Fig. 4. Loss of integrin activation dysregulates EC MAPK signaling

(a) HUVECs were serum-starved and treated with lentiviral shRNA constructs against tln1 (shTln1) or a scramble sequence (shScramble). Deletion of talin1 was efficient and resulted in 70% increase in p-ERK1/2 protein levels relative to shScramble controls as measured by western blotting (**p=.0079). **(b)** MLECs isolated from Tln1 Het and Tln1 L325R adult mice were serum-starved and subject to western blotting to measure p-ERK1/2 levels. Tln1 L325R MLECs had an approximately two-fold increase in p-ERK1/2 levels relative to Tln1 Het controls. (*p=.0454) (P-values listed for individual experiments were generated using Mann-Whitney tests, n=2-5 per group).

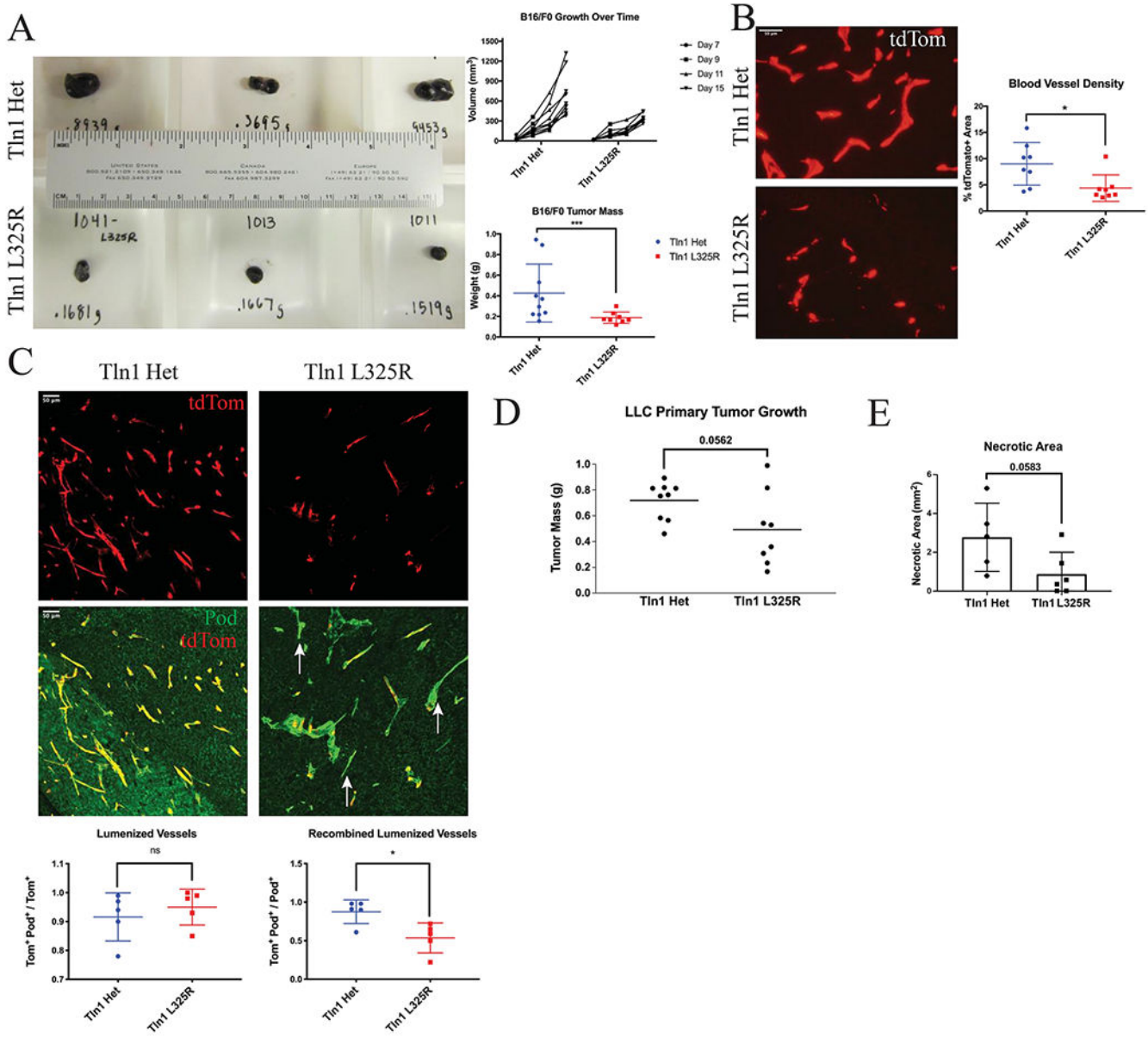

Fig. 5. EC integrin activation is indispensable for primary tumor growth, tumor angiogenesis and vessel lumenization.

(a) B16-F0 tumors were subcutaneously implanted in Tln1 Het and Tln1 L325R adult mice. Tumors were allowed to grow for 14 days with volume measured over time and mass of primary tumor taken on the final day. Tumors grown in Tln1 L325R mice grew slower and were smaller at the final time point relative to Tln1 CTRL mice (***p=.0003) **(b)** Blood vessel density measured by tdTomato+ area in B16-F0 tumor sections from tumors grown in Tln1 L325R and Tln1 Het mice revealed reduced blood vessel density in Tln1 L325R tumor sections. (scale = 50 μm; *p=.0163) **(c)** B16-F0 tumor sections visualized for tdTomato (red) and stained for Podocalyxin (green) and analyzed for Tom+/Pod+ area relative to either total Tom+ area or total Pod+ area from Tln1 L325R and Tln1 Het mice. Although the ratio of Tom+/Pod+/Tom+ areas is comparable, Tln1 L325R tumors have a reduced Tom+/

Pod+/Pod+ areas relative to Tln1 CTRL indicating that most lumenized vessels in Tln1 L325R tumors are non-recombined. (n=5; scale = 50 μm; ns=not significant, *p=.0153) **(d)** Subcutaneously implanted Lewis Lung Carcinoma (LLC) tumors grown for 14 days in Tln1 L325R and Tln1 Het mice phenocopy reductions in primary tumor growth observed in the B16-F0 model. (p=.0562) **(e)** Necrotic area of Tln1 Het and Tln1 L325R B16/F0 tumors was analyzed by H&E staining. Necrotic area is increased in Tln1 L325R tumor sections relative to Tln1 Het (n=5-6 tumors/group; p= .0583) (P-values listed for individual experiments were generated using a 2-tailed unpaired t-test with an n=8-10/group unless otherwise noted).